Cancer Cell
Article

A Hierarchy of Self-Renewing Tumor-Initiating Cell Types in Glioblastoma

Ruihuan Chen,[1] Merry C. Nishimura,[1] Stephanie M. Bumbaca,[1] Samir Kharbanda,[1] William F. Forrest,[2] Ian M. Kasman,[1] Joan M. Greve,[1] Robert H. Soriano,[3] Laurie L. Gilmour,[4] Celina Sanchez Rivers,[3] Zora Modrusan,[3] Serban Nacu,[5] Steve Guerrero,[5] Kyle A. Edgar,[6] Jeffrey J. Wallin,[6] Katrin Lamszus,[7] Manfred Westphal,[7] Susanne Heim,[8] C. David James,[9] Scott R. VandenBerg,[9] Joseph F. Costello,[9] Scott Moorefield,[9] Cynthia J. Cowdrey,[9] Michael Prados,[9] and Heidi S. Phillips[1,9,*]
[1]Department of Tumor Biology and Angiogenesis
[2]Department of Biostatistics
[3]Department of Molecular Biology
[4]Department of Immunology
[5]Department of Bioinformatics
[6]Department of Cancer Signaling
Genentech Inc., San Francisco, CA 94080, USA
[7]University of Hamburg Eppendorf, Hamburg 20246, Germany
[8]Definiens AG, Munich 80339, Germany
[9]Brain Tumor Research Center, University of California San Francisco, South San Francisco, CA 94143, USA
*Correspondence: hsp@gene.com
DOI 10.1016/j.ccr.2009.12.049

SUMMARY

The neural stem cell marker CD133 is reported to identify cells within glioblastoma (GBM) that can initiate neurosphere growth and tumor formation; however, instances of CD133$^-$ cells exhibiting similar properties have also been reported. Here, we show that some *PTEN*-deficient GBM tumors produce a series of CD133$^+$ and CD133$^-$ self-renewing tumor-initiating cell types and provide evidence that these cell types constitute a lineage hierarchy. Our results show that the capacities for self-renewal and tumor initiation in GBM need not be restricted to a uniform population of stemlike cells, but can be shared by a lineage of self-renewing cell types expressing a range of markers of forebrain lineage.

INTRODUCTION

The concept that human malignancies are relentlessly fueled by identifiable subpopulations of tumor cells with unlimited capacity for self-renewal has important therapeutic implications, yet remains a hotly debated issue (Clarke et al., 2006; Sakariassen et al., 2007). Some proponents of the so-called "cancer stem cell theory" suggest that effective therapeutic targeting of self-renewing tumor cells at the apex of a lineage hierarchy might eradicate the capacity for prolonged tumor growth (Korkaya and Wicha, 2007). Human GBM is an aggressive malignancy characterized by marked intra- and intertumoral heterogeneity. Although the neural stem cell marker CD133 has been demonstrated to demarcate GBM cells exhibiting enhanced competencies for self-renewal and tumor initiation (Bao et al., 2006; Singh et al., 2004), instances in which CD133$^-$ cells exhibit similar properties have been reported (Beier et al., 2007; Joo et al., 2008; Ogden et al., 2008; Wang et al., 2008). Because existing studies examining tumor-initiating capabilities of human GBM cells rely on cell-sorting techniques that result in impure cell fractions, it is difficult to draw definitive conclusions on the capabilities of GBM cells as a function of CD133 expression. Thus, it is not clear to what extent GBM cells with the capacity for long-term self-renewal constitute an identifiable subpopulation of tumor cells, much less whether therapeutic targeting of such a population would effectively control the capacity for therapeutic

Significance

Increasing controversy surrounds the concept that identifiable subpopulations of tumor cells exhibiting stem cell properties are selectively critical for the relentless growth of many human malignancies. Our findings establish the importance of *PTEN* status and lineage relationships in determining GBM cell competencies and reveal that individual GBMs can harbor a series of phenotypically distinct self-renewing cell types that promote a range of tumor growth patterns. Importantly, our results demonstrate that individual GBM tumors can contain both CD133$^+$ and CD133$^-$ cell types that generate highly aggressive tumors. These findings suggest that optimal treatment of GBM requires effective targeting of multiple self-renewing tumor cell populations expressing a range of phenotypic markers.

resistance and prolonged tumor growth. Here, we examine heterogeneity of GBM cell competencies for self-renewal and tumor-initiation and the relationship of these properties to cell lineage and molecular markers including CD133 expression.

RESULTS

Tumor *PTEN* Status Correlates with Neurosphere Growth

We began by examining a series of newly diagnosed GBM cases to investigate characteristics of tumor cells that are capable of initiating sustained growth under neural stem cell culture conditions. Twenty-nine newly diagnosed untreated primary GBM tumors were included in this study (Figure 1D; see Figure S1 and Tables S1 and S2 available with this article online). Using flow cytometry, we evaluated tumor cells from surgical specimens for both side population behavior and expression of the stem cell marker CD133. Cells exhibiting side population behavior were rare (<3%) in all cases examined (Table S2). In contrast, flow cytometry revealed a wide range in the fraction of cells expressing CD133 (Figures 1A and 1D), findings that were consistent with qualitative immunohistochemical evaluation (Figure 1B). Surprisingly, expression profiling revealed that GBMs of the poor prognosis *Mesenchymal* subtype (Phillips et al., 2006) contained fewer $CD133^+$ cells (Figure 1C; Tables S1 and S3).

We next sought to determine which molecular features of a tumor correlate with the ability to generate neurosphere cultures. Although all tumors yielded floating aggregates of viable cells in neurosphere culture conditions, only about half of the cultures could be successfully expanded. Cultures that did not increase in cell number within the first three passages invariably failed to ever expand and eventually died. With the exception of culture SF7113, which stopped growing after six passages, all other expandable lines were stably propagated for at least 20 passages. Comparing features of tumors generating successful (n = 16) versus failed (n = 13) neurosphere cultures, no differences were seen in the percentage of $CD133^+$ cells, the percentage of side population cells, patient age, or relative frequencies of the following features: patient sex, expression subtype, MGMT methylation status, p53 mutation, p16 deletion, PDGFR amplification, and EGFR amplification ($p > 0.2$ all comparisons; Figure 1D; Table S2). Patient survival ($p = 0.10$, log rank test) and MIB-1 indices ($p = 0.11$, Student's t test) showed trends for correlation with culture outcome (Figure 1D).

In contrast to the features outlined above, tumor *PTEN* status showed a significant correlation with neurosphere growth (Figure 1D; $p < 0.05$ Fisher's exact probability test, two-tailed). Successful lines were derived exclusively from tumors that exhibited loss or mutation of one or both alleles of *PTEN*. Although 15 of the 23 GBMs with relative copy number loss or mutation of *PTEN* formed successful neurosphere cultures, none of the five GBMs lacking alteration at this locus generated expandable cultures. Consistent with the hypothesis that loss of PTEN function is required for neurosphere growth, all neurosphere lines examined displayed relative loss or mutation at the *PTEN* locus on chromosome 10 (Figure 1E) and reduction or absence of PTEN protein on Western blot (Figure 1F). With one exception, all neurosphere lines were derived from tumors exhibiting relative loss of entire chromosome 10 and retained this alteration. The remaining line, SF7101, and its corresponding tumor displayed homozygous *PTEN* mutation. All lines and their respective tumors exhibited gains of chromosome 7p, but none of the lines derived from patient tumors with *EGFR* amplification retained this alteration (Figures 1D and 1E).

Both $CD133^+$ and $CD133^-$ GBM Cells Initiate Neurosphere Growth

To examine the relationship between CD133 expression and the capacity to initiate neurosphere growth, we utilized fluorescence-activated cell sorting (FACS) and magnetic bead separation to sort $CD133^+$ and $CD133^-$ cell fractions (Figure S2). In all GBMs examined (n = 16), the $CD133^+$ and $CD133^-$ fractions of tumor cells showed qualitatively similar results for neurosphere growth (i.e., both fractions generated expandable neurospheres or both yielded failed cultures) (Figure 1D). To quantify differences in neurosphere initiation capability, we sought to utilize FACS to determine cloning efficiency; however, repeated efforts to clone FACS-sorted tumor cells from patient specimens were unsuccessful. Individual cells (n = 2688) from seven cases yielded no viable clones, in spite of the finding that successful cultures were derived from unsorted cells from four of these cases (Figure 1D). Thus, it appears either that the frequency of clonogenic cells in patient GBM tumors is very low or that procedures associated with dissociation and FACS sorting of patient samples significantly compromise cloning efficiency.

As an alternative source of GBM cells enriched for the capacity to initiate clonal neurosphere growth, we investigated a series of GBM-derived neurosphere lines. Analysis of these neurosphere lines revealed substantial variation in the percentage of $CD133^+$ cells, but this percentage remained constant for individual lines over at least a few passages (Figures 2A and 2C; Figure S3; Table S4). For clonal analysis, a panel of 14 neurosphere lines derived from five human GBM tumors was employed (Figure S1). Included were lines $GS\text{-}2_1$ and $GS\text{-}3_1$, (the products of in vivo passaging neurosphere lines GS-2 and GS-3) (Gunther et al., 2008), three newly generated neurosphere lines ($SF6969_1$, SF7192, and SF7202), and nine sublines of $GS\text{-}2_1$ and $SF6969_1$. Using FACS to clone $CD133^+$ and $CD133^-$ cells, we observed that 13 of the 14 lines yielded viable clones (Figure 2C). Although the panel of lines varied in their frequency of clonogenic cells, no systematic difference was observed in the clonogenicity of $CD133^+$ or $CD133^-$ cells (Figure 2C) or in the appearance of expanded cultures derived from them (Figure 2B). Notably, however, upon dissociation into single cell suspensions, cultures containing $CD133^+$ cells showed much more aggregation than cultures lacking $CD133^+$ cells, whether assayed in the presence (Figure 2D) or absence (data not shown) of the divalent cations calcium and magnesium.

A Series of Three Clonogenic Cell Types Is Identified in GBM

Examining a series of expanded clonal cultures, we identified three clonogenic cell types: Type 1 cells are $CD133^-$ cells that give rise to cultures containing a mixture of $CD133^+$ and $CD133^-$ cells; Type II cells are $CD133^+$ cells that also give rise to mixed cultures; and Type III cells are $CD133^-$ cells that give rise to cultures of only $CD133^-$ cells (Figure 3A). Consistent

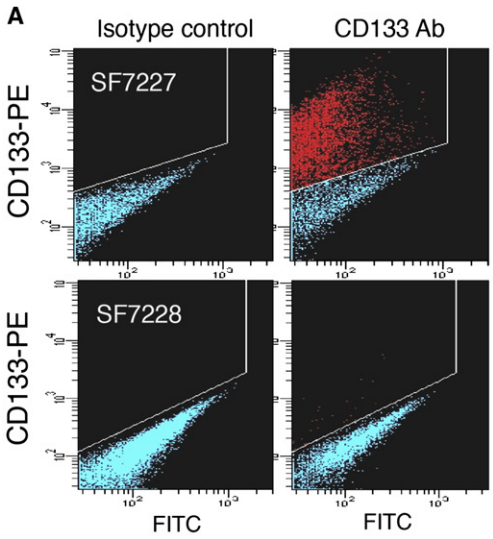

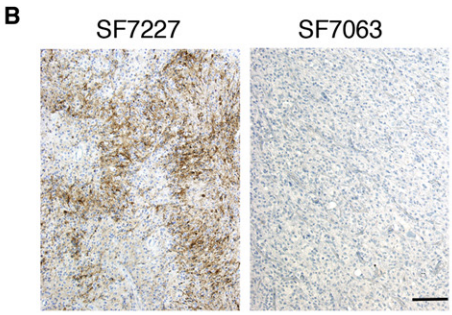

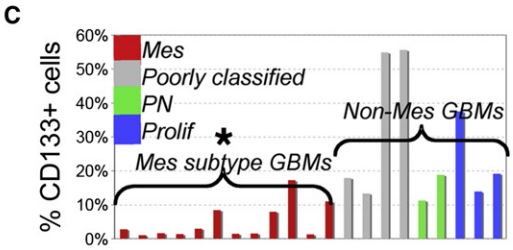

D

Tumor Feature						Neurosphere formation				
Patient ID	Survival	CD133+	MIB1	PTEN	EGFR AMP	unsorted	CD133 + sort	CD133- sort	CD133 + clone	CD133 - clone
SF6977	620	2.7%	12.7%	WT	NC	N	N[1]	N[1]		
SF7029	(921)	1.1%	10.5%	WT	NC	N	N[1]	N[1]		
SF7034	438	1.6%	8.5%	LOSS	AMP	N	N[2]	N[2]		
SF7048	(881)	0.3%	3.1%	WT	NC	N	N[2]	N[2]		
SF7054	676	ND	19.2%	LOSS	AMP	N	N[2]	N[2]		
SF7059	713	ND	16.2%	MUT, LOSS	NC	N				
SF7081	(201)	13.3%	23.7%	LOSS	AMP	N				
SF7082	116	2.9%	22.5%	MUT, LOSS	NC	N				
SF7093	393	37.5%	19.6%	LOSS	NC	N				
SF7180	570	8.4%	7.9%	WT	AMP	N	N[1]	N[1]		
SF7223	447	17.2%	33.7%	MUT, LOSS	AMP	N			N	N
SF7228	224	0.6%	7.3%	WT	NC	N			N	N
SF7284	148	11.0%	35.3%	LOSS	ND	N			N	N
Summary NSP-	*486 +/- 63*	*8.8% +/- 4.7%*	*16.9% +/- 3.0%*	*8/13 altered*	*5/12 AMP*					
SF6969	307	17.9%	33.7%	LOSS	NC	Y	Y[1,2]	Y[1,2]		
SF7030	202	1.0%	1.6%	LOSS	AMP	Y	Y[1,2]	Y[1,2]		
SF7063	510	1.3%	12.1%	LOSS	AMP	Y	Y[1]	Y[1]		
SF7095	134	ND	43.6%	LOSS	NC	Y				
SF7101	233	11.3%	23.6%	HOM MUT	NC	Y				
SF7113	843	18.8%	19.3%	LOSS	NC	Y				
SF7179	35	54.8%	23.3%	LOSS	NC	Y	N[1]	N[1]		
SF7186	265	1.4%	33.1%	LOSS	AMP	Y	N[1]	N[1]		
SF7192	613	8.2%	35.2%	LOSS	NC	Y	Y[1]	Y[1]		
SF7194	493	1.5%	8.2%	LOSS	NC	Y	Y[1]	Y[1]		
SF7201	253	7.9%	ND	LOSS	AMP	Y	Y[1]	Y[1]		
SF7202	476	2.5%	22.1%	ND	ND	Y	Y[1]	Y[1]		
SF7225	387	13.9%	17.1%	LOSS	AMP	Y			N	N
SF7227	542	55.6%	31.5%	LOSS	AMP	Y			N	N
SF7259	(696)	19.1%	31.7%	LOSS	AMP	Y	Y[1]	Y[1]	N	N
SF7276	412	1.2%	17.0%	MUT, LOSS	AMP	Y			N	N
Summary NSP+	*380 +/- 52*	*14.4% +/- 4.6%*	*23.5% +/- 2.9%*	*15/15 altered**	*8/15 AMP*					

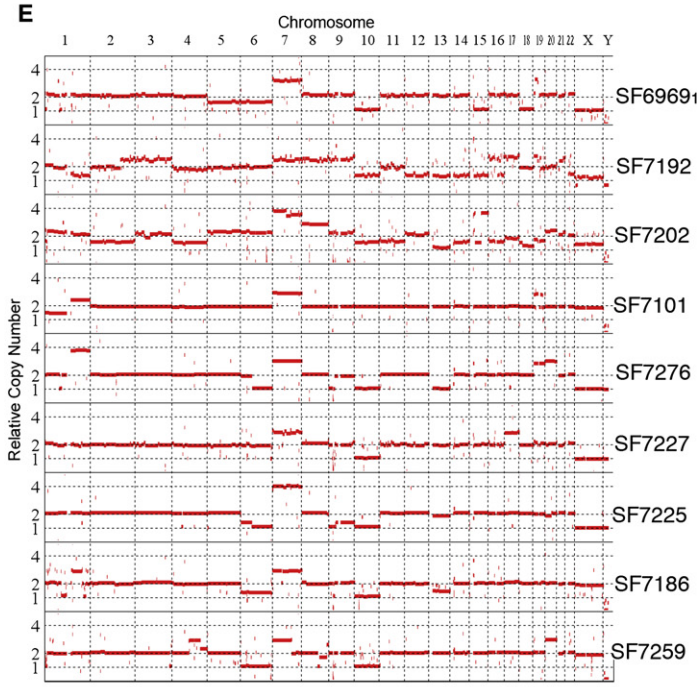

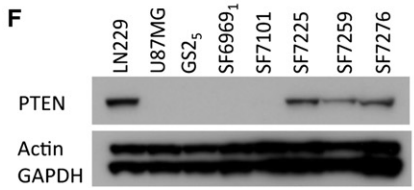

Figure 1. PTEN Status, but Not CD133 Expression, Correlates with Neurosphere Formation

(A) FACS plots of CD133 expression in a patient GBM (SF7227) with an abundance of CD133$^+$ cells and another case (SF7228) with a paucity of cells labeled for CD133. CD133-PE signal (y axis) is plotted against autofluorescence in the FITC channel (x axis). In cells stained with antibody to CD133 (right panels), CD133$^+$ (red) and CD133$^-$ (blue) cells are identified by a FACS gate (white line) established in corresponding isotype control plots (left panels).

(B) Immunohistochemistry for CD133 in two primary GBM specimens found by FACS to contain either high (SF7227) or low (SF7063) percentages of CD133$^+$ cells. Scale bar, 100 microns and applies to both panels (A) and (B).

(C) A smaller percentage of tumor cells express CD133 in *Mesenchymal* (*Mes*) subtype tumors compared to other GBMs including *Proneural* (*PN*) and *Proliferative* (*Prolif*) subtypes and poorly categorized samples (*p = .0007, t test of Mes versus non-Mes).

(D) Characteristics of patient tumors that generate successful (bottom) versus failed neurosphere cultures (top). Summary metrics reported for neurosphere-forming (Summary NSP$^+$) and failed neurosphere (Summary NSP$^-$) patient tumors are mean ± SEM or absolute frequencies. Survival is reported in days; censored values are indicated by parentheses. *PTEN* status is reported as wild-type (WT) if no evidence of mutation (MUT) or loss was seen. ND, not determined.

with detection of CD133 protein by FACS, expression profiling of clones from both tumors SF6969 and GS-2 revealed robust signal for CD133 mRNA in type I and II clones, but very low signal in type III clones (Figure S4). In total, 177 clones from 11 lines representing three patient tumors were profiled by FACS for CD133 expression (Figure 3B). Of the 153 clones for which the presence or absence of $CD133^+$ cells could be unambiguously determined, all but two clones could be classified as type I, II, or III. In total, 25 type I, 67 type II, and 59 type III clones were identified. No clonal cultures contained 100% $CD133^+$ cells, and only two $CD133^+$ cells generated cultures lacking $CD133^+$ cells. Thus, type I, II, and III cells appear to account for nearly all clonogenic cells present in GBM neurosphere cultures.

Not all clonogenic cell types were identified in each of the cultures for which we determined clone phenotypes; although type III cells were seen in all but one culture, type II cells were seen in fewer cultures, and type I cells only occurred in a subset of the cultures that contained type II cells (Figure 3C). The hierarchy of clonogenic cell types present in the series of neurosphere lines suggests the possibility of a lineage relationship between these cell types. Our results demonstrated the presence of all three clonogenic cell types in two of three tumors analyzed. Of note, neurosphere line $GS\text{-}3_1$, which we found to produce only type III clones, was derived from parental line GS-3, a line previously reported to contain $CD133^+$ cells (Gunther et al., 2008). Although line GS-3 has remained positive for content of $CD133^+$ cells in the laboratory of origin, since transatlantic transfer as a live culture, this line has consistently produced cultures and serially transplantable tumors devoid of $CD133^+$ cells. Thus, it is possible that all three clonogenic cell types exist in all GBMs generating neurosphere lines, but loss or irreversible differentiation of type I and II cells can occur.

When maintained in neurosphere media, a substantial fraction of cells in serial-passaged cultures of type I, II, and III clones from both GS-2 and SF6969 were immunopositive for the neural stem cell marker Nestin (Figure 4A). Upon exposure to differentiating conditions, cultures from all clone types displayed a mixture of cells labeling for markers of neurons, astrocytes, and oligodendroglia (Figures 4B, 4C, and 4D). Hence, all three clonogenic cell types have the capability in vitro to generate progeny that express neural stem cell markers and exhibit evidence of multilineage differentiation.

To investigate the self-renewing capacity of the type I, II, and III clonogenic cell types, we conducted secondary cloning experiments. For these analyses, we utilized primary type I, II, and III neurosphere clones derived from patient tumors GS-2 and SF6969. Every clone examined was found to contain cells that initiate growth of secondary clones similar to the initial clone in appearance, growth, and CD133 expression. Secondary clones from $CD133^+$ cells invariably contained a mixture of $CD133^+$ and $CD133^-$ cells, and the percentage of $CD133^+$ cells in these expanded clonal cultures did not differ as a function of the primary clone type from which the secondary clone was derived (Figure 3D). In contrast, for secondary clones derived from $CD133^-$ cells, the content of $CD133^+$ cells varied as a function of the primary clone type, such that type I clones yielded secondary clones with the highest percentage of $CD133^+$ cells, type II clones yielded secondary clones with an intermediate percentage of $CD133^+$, and type III clones yielded secondary clones containing only $CD133^-$ cells (Figure 3D). These findings are consistent with a lineage hierarchy model in which type III cells are relatively differentiated cells incapable of producing $CD133^+$ progeny, whereas both type I and type II cells are more primordial cell types generating a greater diversity of progeny.

To assess the capability of each clone type for prolonged growth in vitro, we selected a series of type I, II, and III clones derived from patient tumor GS-2 and propagated each line for greater than 20 passages. No differences in growth rate or appearance of the lines were observed as a function of clone type, and all lines continued to show stable propagation for as long as they were observed. Repeated FACS profiling of these clonal neurosphere lines revealed that cultures of type III clones invariably produced only $CD133^-$ cells, whereas, with one exception, all type I and II lines maintained a mixture of $CD133^+$ and $CD133^-$ cells (Figure 3E).

Type I, II, and III Cells Generate Tumors with Different Growth Kinetics

Having identified the presence of three cell types capable of long-term propagation and serial clonogencity in vitro, we examined the ability of progeny from each of these cell types to generate orthotopic tumors in nude mice. For these studies, we utilized the same clonal lines derived from patient tumor GS-2 that were used for long-term in vitro profiling in Figure 3E. Because tumor SF6969, the second GBM case for which we identified all three self-renewing cell types, generated a parental neurosphere line and sublines that were not tumorigenic (data not shown), we did not examine tumorigenicity of clonal lines derived from this tumor.

A series of mice, each inoculated in the forebrain with 10^5 cells from a GS-2 clonal line, were monitored by magnetic resonance imaging (MRI) 12 weeks after implantation. Although most mice grafted with type I or II clones harbored sizeable lesions at this time point, most mice implanted with type III clones showed no evidence of tumor (Figures 5A and 5B). Importantly, however, MRI monitoring at later intervals revealed that all of the clones eventually generated detectable lesions and, by eight months after implantation, tumors arose in all mice inoculated that did not die of unrelated causes (Figure 5A; Table S5). Replicate grafts of each clone showed a great deal of consistency, and tumor volumes varied significantly as a function of clone type,

Tumor SF7101 showed homozygous mutation (HOM MUT) associated with isodisomy of chromosome 10. Ability to form expandable neurosphere cultures is designated Y for successful cultures and N for failed cultures. Neurosphere expansion was determined for unsorted tumor cells (unsorted), bulk $CD133^+$ and $CD133^-$ populations ($CD133^+$ sort, $CD133^-$ sort), and single $CD133^+$ and $CD133^-$ cells cloned by FACS ($CD133^+$ clone, $CD133^-$ clone). For bulk-sorted populations, results from FACS sorting are denoted by the superscript 1, and magnetic bead separations by superscript 2.

(E) Relative DNA copy number estimates of neurosphere lines as determined by array CGH. All lines displayed relative copy number losses of chromosome 10 except SF7101.

(F) Western blot for PTEN protein reveals reduced signal in neurosphere cultures (as labeled) compared to LN229, an adherent line homozygous for wild-type *PTEN*. (See also Tables S1, S2, and S3; Figure S2.)

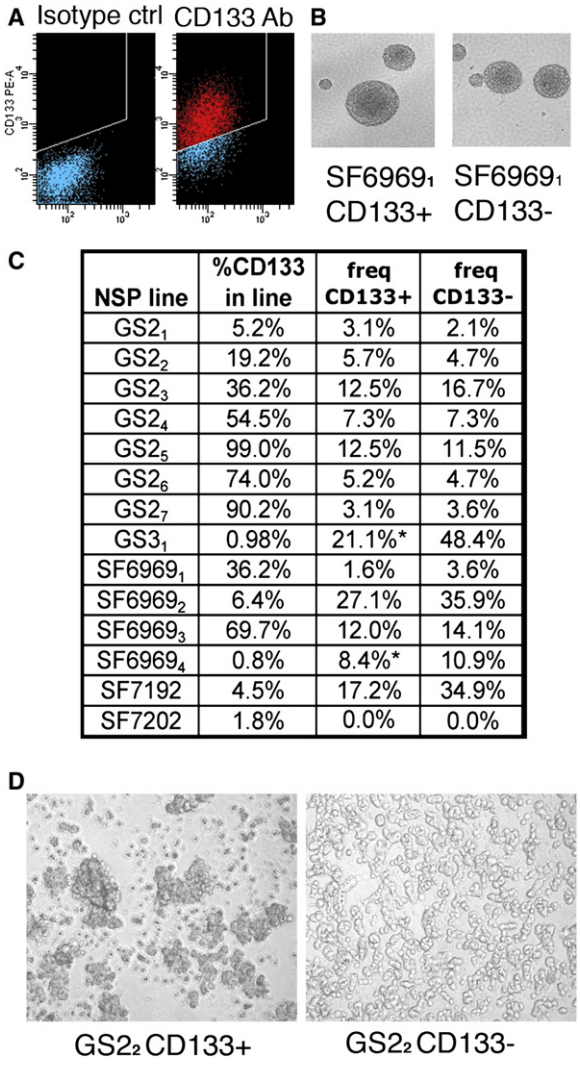

NSP line	%CD133 in line	freq CD133+	freq CD133-
GS2$_1$	5.2%	3.1%	2.1%
GS2$_2$	19.2%	5.7%	4.7%
GS2$_3$	36.2%	12.5%	16.7%
GS2$_4$	54.5%	7.3%	7.3%
GS2$_5$	99.0%	12.5%	11.5%
GS2$_6$	74.0%	5.2%	4.7%
GS2$_7$	90.2%	3.1%	3.6%
GS3$_1$	0.98%	21.1%*	48.4%
SF6969$_1$	36.2%	1.6%	3.6%
SF6969$_2$	6.4%	27.1%	35.9%
SF6969$_3$	69.7%	12.0%	14.1%
SF6969$_4$	0.8%	8.4%*	10.9%
SF7192	4.5%	17.2%	34.9%
SF7202	1.8%	0.0%	0.0%

Figure 2. CD133$^+$ and CD133$^-$ GBM Neurosphere Cells Are Equally Clonogenic

(A) Representative FACS plot of CD133 expression in a neurosphere line (GS-2$_4$). In the right panel, CD133$^+$ (red) and CD133$^-$ (blue) cells of GS-2$_4$ are identified by a gate (white line) established using an isotype control plot of the same culture (left panel).

(B) Clones Expanded from a CD133$^+$ and a CD133$^-$ cell from line SF6969$_1$.

(C) Clonogenic frequency in a series of neurosphere lines. Percentage of CD133$^+$ cells in each line is reported, as well as the percentages of CD133$^+$ and CD133$^-$ cells cloned by FACS that yielded a neurosphere (freq CD133$^+$, freq CD133$^-$, respectively). *Results from cloning the rare population of cells residing in the CD133$^+$ sort window are reported even though these two parental lines and all expanded clones were deemed to have no CD133$^+$ cells.

(D) Dissociated cells from clonal cultures assayed for aggregation in the presence of calcium and magnesium. Cell aggregates are larger in the culture containing CD133$^+$ cells (left) compared to containing only CD133$^-$ cells (right). (See also Figure S3 and Table S4.)

such that type I was greater than or equal to type II, which was greater than type III (Figure 5B). Histological analysis of mice killed shortly after MRI demonstrated a good correspondence for all three clone types between areas quantified as tumor on T2-weighted MR images and regions of high tumor cell content in tissue sections (Figure S5). We next repeated the tumor initiation experiment using a series of type I, II, and III secondary clones derived from a single primary type I clone. Tumors arose in all mice inoculated, and the pattern of tumor volumes as a function of clone type was very similar to that seen in the first experiment (Figure 5C). Thus, in this experiment with established lineage relationships between clonal lines, growth kinetics vary as a function of clone type. These results show that a single CD133$^-$ cell (type I) is capable of producing phenotypically distinct progeny (type I, II, or III) that initiate tumors with a wide range of growth kinetics. Repeated volumetric assessments of grafts from secondary clones revealed that type III tumors expanded more slowly than did type I or II lesions (Figure 5D).

Type I, II, and III Clones Support Serial Transplantation

Grafts from type I (n = 2), type II (n = 1), and type III (n = 2) clonal lines all demonstrated 100% tumorigenicity when serially transplanted (Figure 5E; Table S6). For both primary and serial transplants, tumors harvested from mice inoculated with type I or II lines generated neurosphere cultures that contained a mixture of CD133$^+$ and CD133$^-$ cells, whereas tumors harvested from grafts of type III lines gave rise to cultures that contained only CD133$^-$ cells (Figure 5F). Thus, each of the three clonogenic cell types supports self-renewal in vivo, although type III clones reconstitute more limited aspects of the original tumor.

Type I, II, and III Cells Generate Grafts with Distinct Histological Features

Histological analysis of grafts arising from the three clone types revealed distinct features associated with each. Grafts of type III clones grew with sharp borders between tumor and surrounding host brain (Figure 6C). Invasion of these grafts occurred as fingerlike masses of tumor cells projecting into brain parenchyma or as tumor cells invading along perivascular spaces (Figure 6C). In contrast, grafts from type I and II lines displayed diffuse borders between tumor and brain (Figures 6A and 6B). These grafts produced single tumor cell infiltrates into both brain parenchyma and along white matter tracts, and tumor cells were more rarely seen to invade perivascular spaces. A notable feature of type I grafts was elongated tumor cells (Figure 6A), a feature that was significantly more frequent in type I than type II or III grafts (Figure 6D). Surprisingly, proliferation indices of type III clone grafts were higher than that of type I grafts (Figure 6E). None of the grafts displayed evidence of microvascular proliferation, a feature common to all GBMs and especially prominent in *Mesenchymal* subtype GBMs (Phillips et al., 2006). Consistent with the histological findings, expression profiling revealed that none of the clone grafts resembled *Mesenchymal* subtype patient tumors and that type III grafts showed more *Proliferative* character than type I grafts (Table S7).

Type I, II, and III Cells Generate Grafts with Distinct Molecular Signatures

Principal component analysis using genes that differed consistently across clone types in GS-2 and SF6969 clonal cultures revealed that, for both tumors, the first principal component stratified clones in a continuous fashion such that type I and III clones populate the ends of a spectrum and type II clones

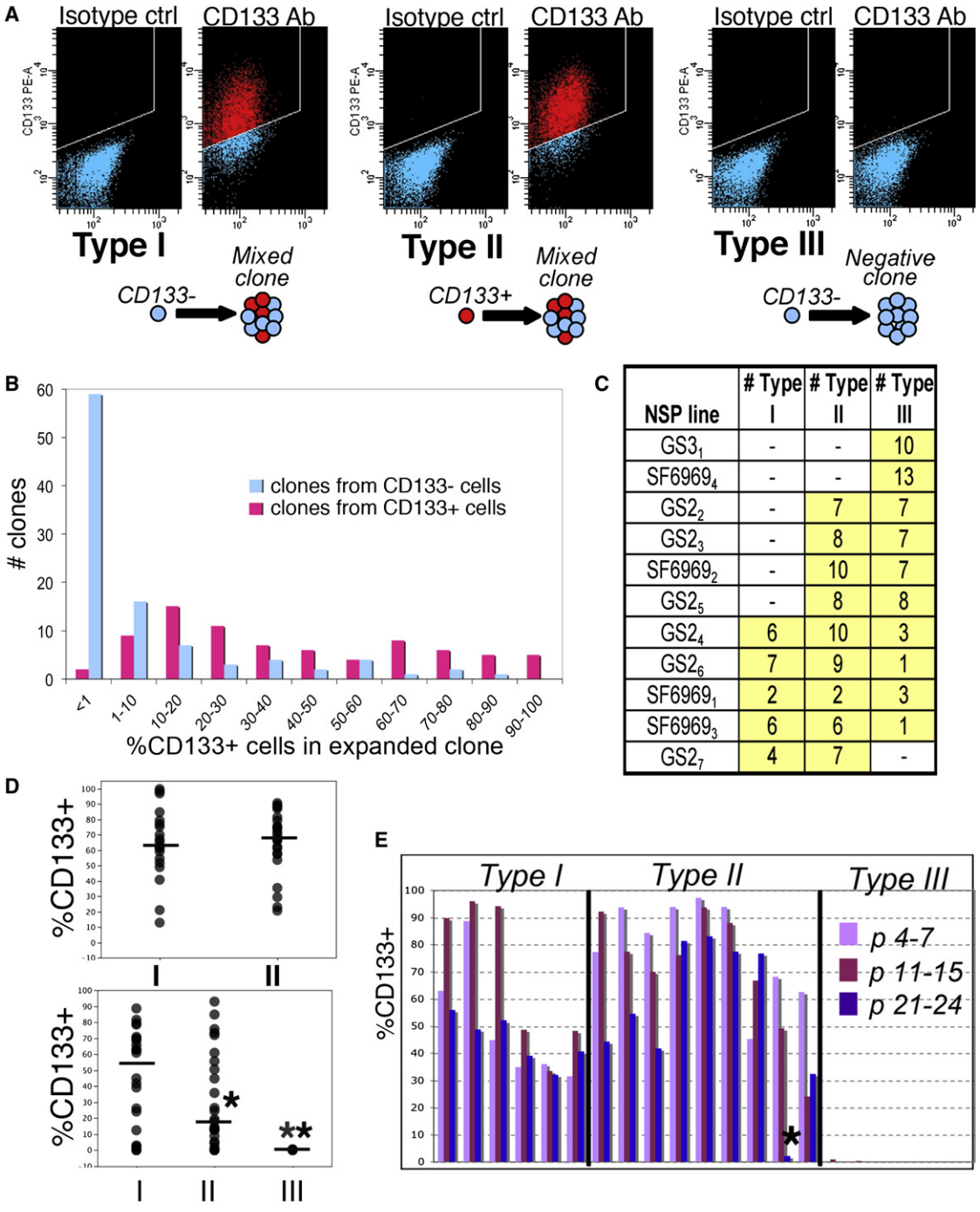

NSP line	# Type I	# Type II	# Type III
$GS3_1$	-	-	10
$SF6969_4$	-	-	13
$GS2_2$	-	7	7
$GS2_3$	-	8	7
$SF6969_2$	-	10	7
$GS2_5$	-	8	8
$GS2_4$	6	10	3
$GS2_6$	7	9	1
$SF6969_1$	2	2	3
$SF6969_3$	6	6	1
$GS2_7$	4	7	-

Figure 3. Three Clonogenic Cell Types Are Identified in GBM Cases

(A) FACS plots of type I, II, and III clones derived from the parental line shown in Figure 2A. Type I and II cells are $CD133^-$ and $CD133^+$ cells, respectively, which gave rise to a mixture of $CD133^+$ and $CD133^-$ cells. Type III cells are $CD133^-$ cells, which give rise to only $CD133^-$ cells.

(B) Frequency of primary clones as a function of the percentage of $CD133^+$ cells in the expanded clonal culture. Blue bars represent clones expanded from $CD133^-$ cells, whereas pink bars represent clones expanded from $CD133^+$ cells.

(C) Frequency of type I, II, and III cells identified in a series of neurosphere lines.

(D) Percentage of $CD133^+$ cells in secondary clones as a function of the cell type cloned. Top panel depicts secondary clones of $CD133^+$ cells cloned from type I or II primary clones, and bottom panel displays secondary clones expanded from $CD133^-$ cells from type I, II, or III primary clones. $^{**}p < 0.0005$ type III versus I; $^{*}p < 0.05$ for both type II versus I and type II versus III (t tests with Holm's correction for multiple comparisons). Bars represent median values.

(E) Percentage of $CD133^+$ cells in a series of clonal lines assayed at three different in vitro passage (p) numbers. Asterisk denotes a type II line that became negative for $CD133^+$ cells after passage 21. Less than 1% $CD133^+$ cells were seen for all type III clonal lines (n = 6) at all passages. (See also Figure S4.)

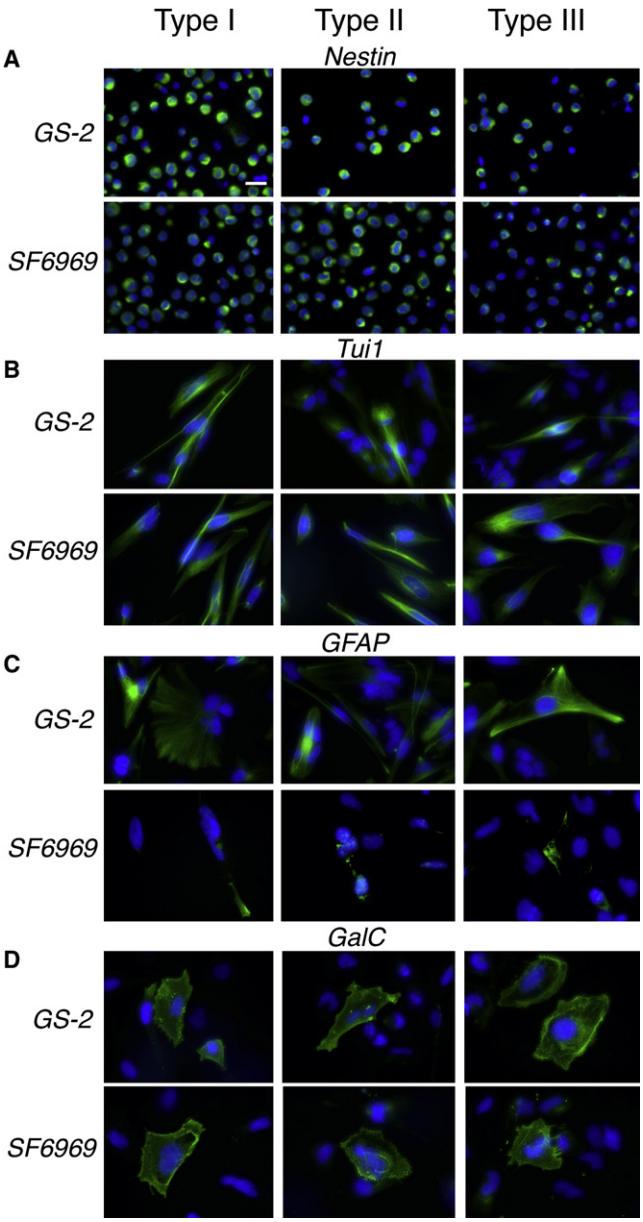

Figure 4. Type I, II, and III Clones Support Multilineage Differentiation

(A) When maintained in neurosphere growth conditions, type I, II, and III clones from both GS-2 and SF6969 display a substantial fraction of cells expressing Nestin.

(B–D) Under differentiating conditions, all clonal cultures contain cells that label for GFAP, TUJ1, and GalC (as indicated). SF6969 clonal cultures exposed to differentiation media produced a predominance of $TUJ1^+$ cells along with smaller numbers of $GFAP^+$ and $GalC^+$ cells, whereas GS-2 clones produced substantial numbers of both $GFAP^+$ and $TUJ1^+$ cells and smaller numbers of $GalC^+$ cells. For (A)–(D), bar in upper left panel is 0.025 mm, green signal represents immunopositivity, and blue signal is DAPI nuclear counterstain.

occupy an intermediate position (Figures 7A and 7B; and Figure S6A). Analysis of grafts from GS-2 revealed that, once again, the type II clones were intermediate between extremes set by type I and III clones (Figures S6B and S6C). These findings are consistent with a lineage model in which type I cells are the most primitive progenitor for self-renewing cell types in GBM and type III cells are the most differentiated self-renewing cell type (Figure 8).

For GS-2 clones, differences in gene expression as a function of clone type were notably more robust in grafts than cultures (Table S8). One gene most differentially expressed among graft types is FABP7 (or BLBP), a radial glial marker that has been previously associated with invasiveness and poor outcome in GBM (Kaloshi et al., 2007; Liang et al., 2006) and that is a marker of tumor-initiating cells in ependymoma (Taylor et al., 2005). Grafts of both type I and II clones express high levels of FABP7, whereas expression in type III grafts is much lower (Figure 7C). Immunohistochemistry confirmed strong expression of FABP7 in grafts of type I and type II clones, and, within these grafts, expression was particularly intense in elongated invading tumor cells (Figure 5A), which presented images resembling radial glia. Comparing expression of a series of markers of neural stem cells (Ghashghaei et al., 2007; Noctor et al., 2007) in type I versus type III grafts, we find that type I grafts express higher levels of FABP7, Nestin, GLAST, and Vimentin and show a nonsignificant trend for overexpression of SOX2 (Figure 7C). In contrast, type III grafts show significantly higher expression of markers of intermediate progenitors (Iulianella et al., 2008; Nieto et al., 2004; Noctor et al., 2007) including TBR2, DLX2, DLX1, and CUTL2, (Figure 7D). For markers of both neural stem cells and intermediate progenitors, type II grafts typically showed expression values that fell within the extremes set by type I and III grafts (Figures 7C and 7D).

DISCUSSION

The current investigation relates heterogeneity of GBM cell capabilities to cell lineage and molecular markers, including but not limited to, CD133 expression. Our results indicate that *PTEN* status and cell lineage appear to be key determinants of GBM cell capabilities and reveal that individual GBMs can contain a series of self-renewing tumor-initiating cells that exhibit a range of phenotypic markers and in vivo growth patterns.

Previous studies have indicated that neurosphere cultures grow from only a subset of GBMs (Galli et al., 2004; Gunther et al., 2008), and that the ability to generate successful neurosphere lines is negatively correlated with patient survival time (Pallini et al., 2008). These studies suggest that specific molecular subtypes of GBM are enhanced in the ability to grow in neural stem cell culture conditions, but they do not provide insight into the molecular determinants of this competency. Of the characteristics we examined in a series of newly diagnosed GBM cases, *PTEN* deficiency was the only statistically significant correlate of successful neurosphere propagation. Although nearly two-thirds of the *PTEN*-deficient cases in our study generated expandable neurosphere lines, none of the five GBMs with both *PTEN* loci intact generated successful cultures. These results suggest that *PTEN* insufficiency may be required to facilitate GBM cell growth in neurosphere conditions, but the failure of some *PTEN*-deficient GBMs to generate successful cultures may indicate necessity of additional molecular determinants. Our finding that *PTEN*-deficient GBM tumors are enhanced for the ability to propagate neurosphere lines is paralleled by findings that *PTEN* deletion enhances self-renewal and

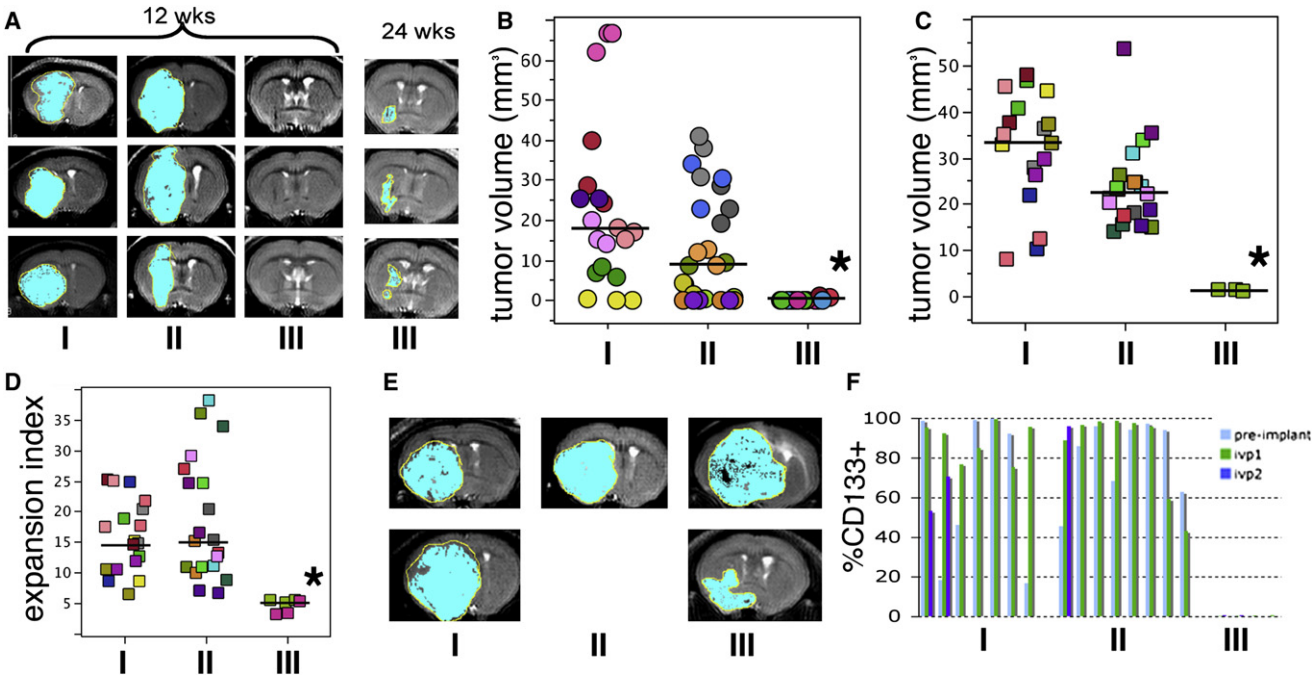

Figure 5. Clone Types Generate Orthotopic Grafts with Different Growth Kinetics

(A) Representative MR images show that grafts of type I and II clones are visible at 12 weeks after implantation, whereas lesions from type III clones are typically not apparent at 12 weeks and small at 24 weeks. Blue pseudocoloring highlights tumor area.

(B) At 12 weeks after implantation, tumor volumes are smaller for type III grafts than either type I or type II grafts (*$p < 0.05$ for both comparisons, Bonferroni corrected p values from Wilcoxon two-sample exact tests). For (B)–(D), results from replicate mice ($n = 2$ or 3) are displayed by symbols of the same color, and bars indicate median values.

(C) For a series of secondary clones derived from one primary type I clone, tumor volumes at 12 weeks after implantation are smaller for grafts of type III clones than grafts of either type I or type II clones (*$p < 0.00005$ for both comparisons, Bonferroni corrected t tests; $p < 0.00001$ for overall effect of clone type, F-test from linear mixed model).

(D) Type III grafts expand more slowly than do type or type II grafts (*$p < 0.0005$ for both I versus III and II versus III, Bonferroni corrected t tests; $p < 0.00005$ for overall clone effect, F-test from a linear mixed model). Expansion index represents the fold change in tumor volumes over a six-week period. Measurements were initiated at six weeks for type I and II grafts and 12 weeks for type III grafts.

(E) Representative MR images of serial transplants of two type I clones, one type II clone, and two type III clones.

(F) Percentage of $CD133^+$ cells in neurosphere lines prior to implantation (preimplant) or following the first or second in vivo passage (ivp1, ivp2). A mixture of $CD133^+$ and $CD133^-$ cells was derived from type I and II grafts, whereas type III grafts ($n = 4$) generated exclusively $CD133^-$ cells. (See also Tables S5 and S6 and Figure S5.)

proliferation of both adult and embryonic neural stem cells (Gregorian et al., 2009; Groszer et al., 2001) and cooperates with *p53* loss in neural stem cells to promote an undifferentiated state with high renewal capacity and tumorigenic potential (Zheng et al., 2008). Additional support for the role of *PTEN* status in determining GBM cell capabilities comes from a series of reports demonstrating that *PTEN* deletion enhances the formation of aggressive high-grade lesions and neurosphere-forming capacity in genetically engineered mouse models of glioma (Bleau et al., 2009; Kwon et al., 2008; Wei et al., 2006; Xiao et al., 2002). Of note, haploinsufficiency of *PTEN* is sufficient to drive effects in both neural stem cells and glioma models (Groszer et al., 2001; Kwon et al., 2008; Xiao et al., 2002).

Our observations of patient tumors indicate that the frequency of GBM cells expressing the stem cell marker CD133 does not correlate with the ability of dissociated cells from a tumor to grow in neurosphere culture conditions. The finding that GBMs of the poor prognosis *Mesenchymal* expression subtype contain fewer $CD133^+$ cells is similar to that of a recent report (Joo et al., 2008), and suggests the possibility that the poor prognosis of some GBMs may be related to tumor growth that is not fueled by $CD133^+$ cells. This suggestion is supported by our clonal analysis revealing populations of GBM-derived $CD133^-$ cells that support long-term growth and self-renewal in vitro and can initiate serially transplantable tumors.

A major finding of the current investigation is that both $CD133^+$ and $CD133^-$ cells from the same GBM tumor can exhibit self-renewal in vitro and the capability to generate serially transplantable tumors in immunocompromised mice. Our findings confirm both the observation that CD133 is a marker for self-renewing tumor-initiating GBM cells (Singh et al., 2004) and the suggestion that, in some instances, $CD133^-$ cells can share these properties and even give rise to $CD133^+$ cells (Beier et al., 2007; Ogden et al., 2008; Wang et al., 2008). Our observation that dissociates of cultures derived from $CD133^+$ cells show greater aggregation than suspensions of cultures containing only $CD133^-$ cells indicate that caution should be exerted in interpreting the behavior of bulk-sorted cell populations. By utilizing

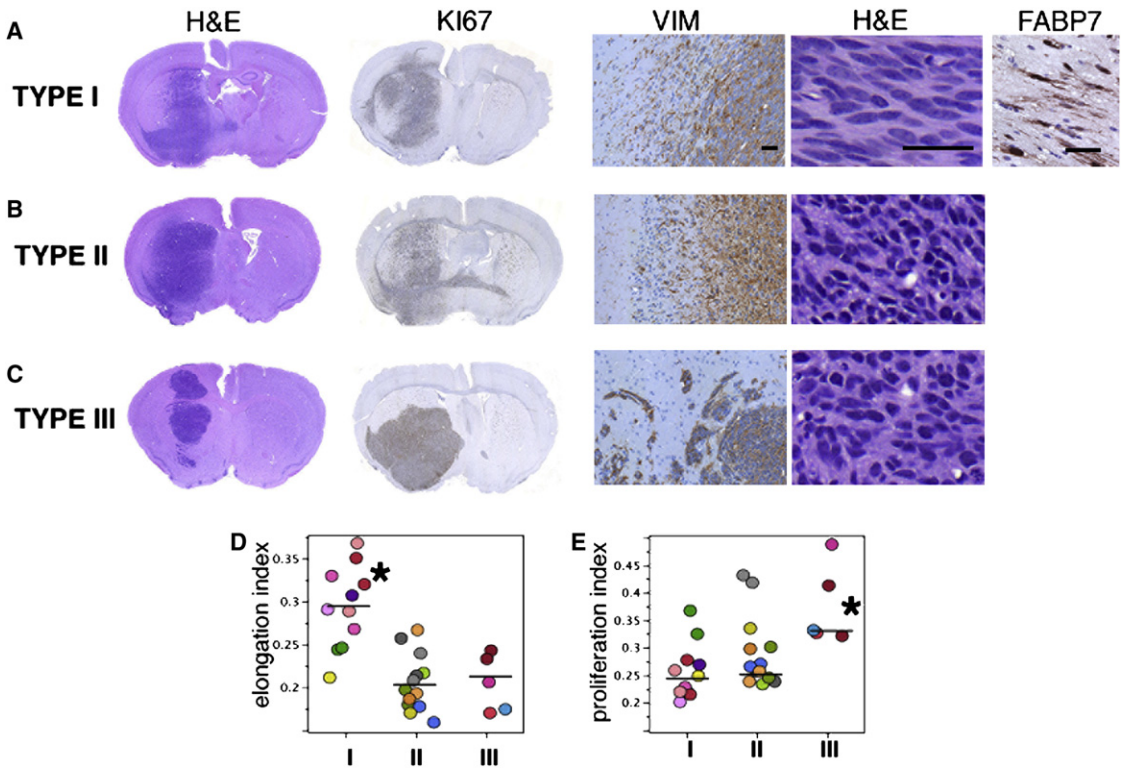

Figure 6. Clone Types Generate Grafts with Distinct Histologies

Histology of type I (A), type II (B), and type III (C) clone grafts. Stains depicted are hematoxylin and eosin (H&E), as well as immunohistochemistry for Ki67, FABP7, and Vimentin (VIM). Scale bars in (A) are 0.05 mm and pertain to corresponding panels in (B) and (C).

(D) Type I grafts have a greater fraction of elongated cells than do either type II or III grafts (*$p < 0.005$ for both comparisons, t tests with Bonferroni correction; $p < 0.0005$ overall effect of clone type, F-test from a linear mixed model).

(E). Type III grafts have a greater fraction of Ki67 positive cells than do type I grafts (*$p < 0.05$, Bonferroni corrected t test; $p < 0.01$for overall clone effect, F-test from a linear mixed model). Bars in (D) and (E) indicate median values and results from replicate mice are displayed by symbols of the same color. (See also Table S7.)

FACS cloning, we have been able to describe the intrinsic capabilities of individual tumor cells and their progeny.

The model we propose (Figure 8) on the basis of our clonal analysis suggests that patient tumors contain multiple distinct populations of lineally related CD133$^-$ cells representing different stages of differentiation: type I cells (which generate aggressive tumors comprising a mixture of CD133$^+$ and CD133$^-$ cells), type III cells (which give rise to slow-growing circumscribed lesions of CD133$^-$ cells), and a third population of CD133$^-$ cells that does not thrive under neurosphere conditions and may not be tumorigenic. Differences in the proportions of these populations of CD133$^-$ cells between patient tumors could provide an explanation for the discrepancies among previous reports about the abilities of CD133$^-$ cells isolated directly from patient tumors or xenografts to form neurospheres or tumors (Beier et al., 2007; Joo et al., 2008; Ogden et al., 2008; Singh et al., 2004; Wang et al., 2008). Importantly, our model predicts that relative enrichment of self-renewing tumor-initiating cell types in neurosphere culture allows these cultures to reveal populations of self-renewing CD133$^-$ cells that could be masked by differentiated populations of CD133$^-$ cells present in bulk-sorted CD133$^-$ cell fractions from patient tumors. Additional studies are needed to determine whether all self-renewing cell types we report occur in all patient tumors and to determine molecular markers that are unique to subclasses of CD133$^-$ GBM cells with differing competencies.

Although alternate models are plausible, several sets of observations support the idea that type I, II, and III cells constitute a lineage of self-renewing cells wherein type I and III cells (both of which are CD133$^-$) represent the most primordial and differentiated states, respectively (Figure 8). Specifically, type II clones are intermediate between the extremes set by type I and III clones in the following features: (1) presence of the cell types across the series of neurosphere lines investigated; (2) percentage of CD133$^+$ cells in secondary clones derived from CD133$^-$ cells; (3) growth kinetics of orthotopic grafts; (4) frequency of elongated tumor cell profiles in grafts; and (5) gene expression profiles. Although the model we propose suggests that type I cells represent progenitors of type II cells, our data do not allow us to distinguish between this possibility and one in which type I and II cells represent inter-convertible phenotypic states of the same cell population. The demonstration that CD133 expression can vary as a function of cell cycle (Jaksch et al., 2008) suggests the possibility that type I and II cells might represent different stages of a single cell type. This suggestion is not, however, consistent with the observed

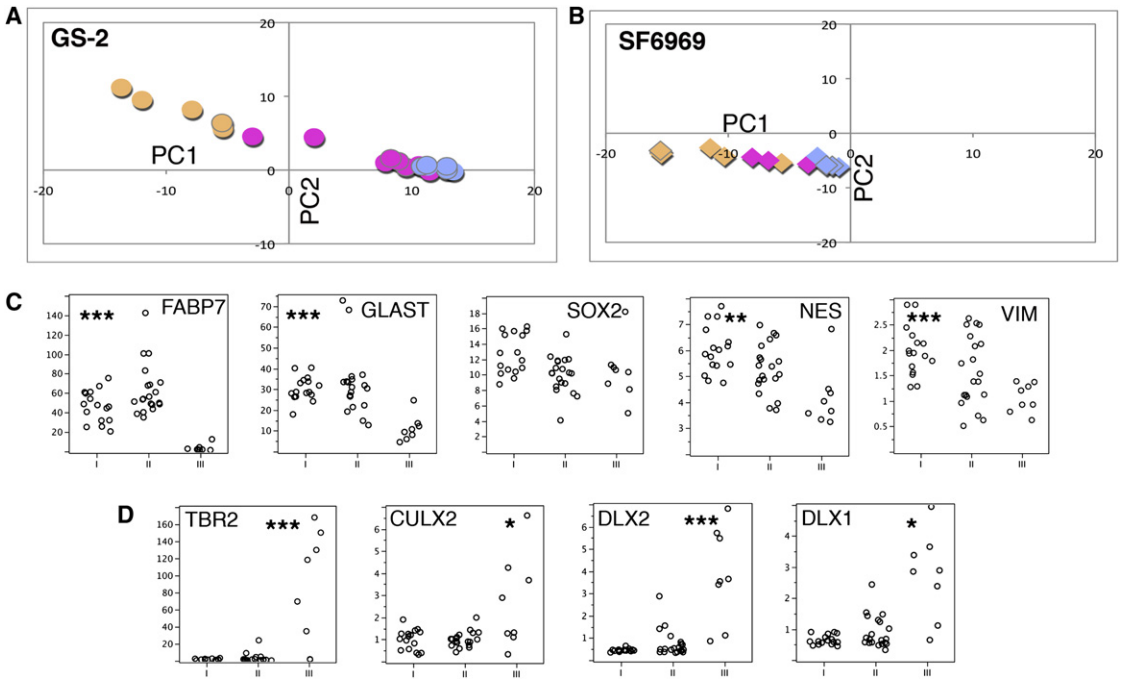

Figure 7. Clone Types Display a Spectrum of Gene Expression

(A and B) Principal component analysis for cultures of clones from GS-2 (A) or SF6969 (B) stratifies clone types as a function of the first principal component (PC1). Analysis was performed using a list of 156 genes whose expression changed coordinately across clone types from both tumors. Similar results were seen if clustering was performed with greater numbers of genes (Figure S6). Orange, pink, and blue symbols represent type I, II, and III clone grafts, respectively.

(C) Expression of four out of five neural stem cell markers is higher in type I grafts than type III grafts.

(D) Intermediate progenitor markers are more highly expressed in type III versus type I grafts. For (C) and (D), *p < 0.05, **p < 0.005, and ***p < 0.0005, for type I versus type III. (See also Figure S6 and Table S8.)

differences in both gene expression and histology of grafts generated from type I and II clone types. Regardless of the exact relationship between type I and II cell types, our data provides compelling evidence that type I cells represent a population of $CD133^-$ cells that is capable of generating a mixture of $CD133^+$ and $CD133^-$ cells in vitro and, in at least the one GBM case tested, is highly tumorigenic. In addition, our data clearly demonstrate that type I and II cells, both of which produce $CD133^+$ and $CD133^-$ cells, are progenitors for type III cells, a population of self-renewing cells that produces only $CD133^-$ cells.

In the grafts of clonal lines from patient tumor GS-2, we observed striking differences in growth patterns and gene expression as a function of clone type. Gene expression patterns of grafts stratified clones by type, but did so in a continuous fashion. Although differences in gene expression between clone types were more modest in vitro, the expression of genes that varied consistently across clone types stratified cultures of both GS-2 and SF6969 clones in a pattern similar to that seen for the grafts. These findings suggest that each clone may generate progeny that tend to persist at a particular stage along a differentiation hierarchy and that the self-renewing cell types we describe each represent a range along a continuum of phenotypes. Of particular interest is our finding that both type I and type II clonal lines generate rapidly growing invasive grafts that express radial glial markers including FABP7, whereas grafts of type III clonal lines give rise to slow-growing circumscribed lesions that express markers of intermediate progenitors, a more differentiated cell type in the forebrain neural lineage. These findings are consistent with previous reports that link FABP7 to invasive behavior and poor prognosis in GBM (Kaloshi et al., 2007; Liang et al., 2006) as well as to proliferation and maintenance of stem cell phenotype in forebrain development (Arai et al., 2005). Because markers of human forebrain lineage have not been thoroughly described, the ability to explore parallels between the phenotype of our clone type grafts and cell types in human forebrain lineage is limited; hence, our conclusions relating clone types to differentiation are tentative.

An important limitation of the current study is that our analysis of self-renewing cell types in GBM pertains only to the subset of GBMs containing cells that can be propagated in neurosphere culture conditions. Recent work in a mouse model of medulloblastoma indicates tumor-propagating capabilities of cells that lack neurosphere-generating capacity (Read et al., 2009). Hence, our observations do not preclude the possibility that cell types capable of long-term self-renewal and tumor initiation in vivo were not identified in our study. In particular, we note that none of the orthotopic neurosphere grafts in this study or in our previous work (Gunther et al., 2008) reconstitute tumors with microvascular proliferation or a *Mesenchmyal* signature. In addition, we cannot say to what extent our observations on tumor growth properties for type I, II, and III clonal lines derived from patient tumor GS-2 are representative of the behavior of self-renewing cell types from other patient tumors. Our observations

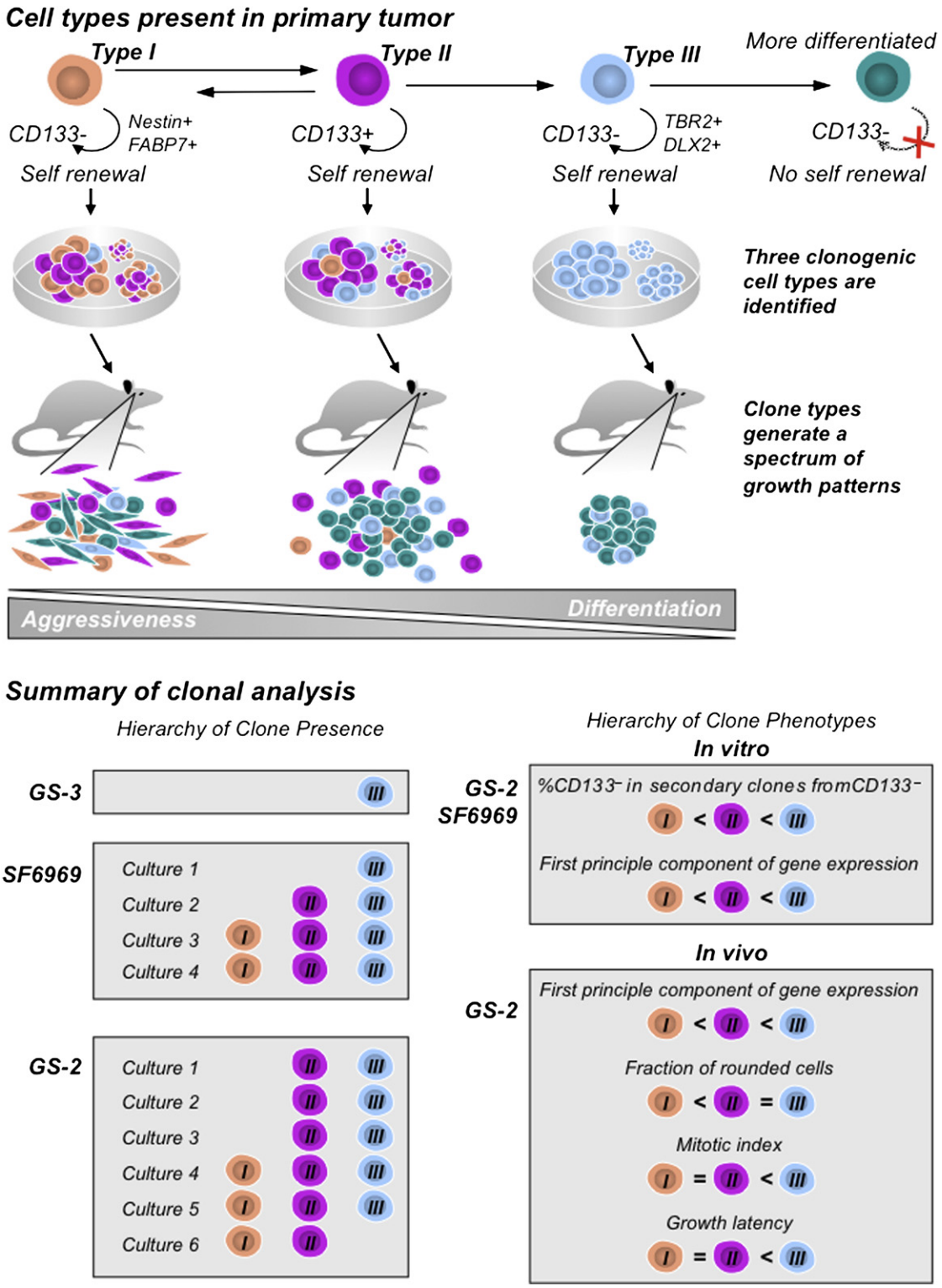

Figure 8. Lineage Hierarchy Model of Type I, II, and III Cell Types

The model depicted in the upper portion of this figure demonstrates how clonogenic cell types present in neurosphere lines may relate to cell types in patient tumors, whereas the lower portion of the figure is a schematic summary of data from clonal analysis of tumors GS-2, GS-3, and SF6969. (See also Figure S1.)

do, however, indicate unequivocally that individual GBMs can contain a hierarchy of self-renewing tumor cells capable of promoting growth of a spectrum of serially transplantable tumor phenotypes.

It is important to recognize that the current results relating cell lineage to tumor cell capabilities pertain to relationships among cells of established tumors and do not speak to the issue of cell type of origin for GBM. Results from genetically engineered models have demonstrated that medulloblastomas or gliomas can be driven by the introduction of mutations into either neural stem cells or lineage committed cell types, and that tumor phenotypes can be very similar for tumors arising from these different cell types (Dai et al., 2001; Read et al., 2009; Schuller et al., 2008; Uhrbom et al., 2002; Yang et al., 2008). Recent results from a somatic tumor suppressor model of astrocytoma provide clear evidence that lesions arising from manipulated neural stem cell/progenitors generate both tumor cells expressing neural stem cell markers as well as tumor cells expressing markers of both differentiated neuronal and glial lineages (Alcantara Llaguno et al., 2009). Interestingly, transplantation experiments of a medulloblastoma model convincingly demonstrate that cells expressing the progenitor marker CD15, but not the neural stem cell marker CD133, are capable of tumor propagation (Read et al., 2009). Thus, although the phenotype of cells present in a tumor may not be a direct reflection of cell type of origin, in at least some instances, tumor cell capabilities do appear to vary as a function of lineage relationships among tumor cells.

Our findings add to the growing body of evidence that lineage relationships of cells within a solid human tumor can be an important determinant of tumor cell competencies, but suggest that cells expressing a range of differentiation markers can contribute to the relentless and aggressive growth of individual malignancies. These findings predict that therapeutic approaches targeting individual stem cell markers may confer limited benefit and provide impetus for strategies to address phenotypically diverse populations of self-renewing tumor cells.

EXPERIMENTAL PROCEDURES

Patient Tumors

This study was approved by the Committee on Human Research of the University of California San Francisco, and all patients signed an approved consent document prior to surgery. Surgical specimens of tumors were examined by a neuropathologist to verify that each case met WHO criteria for GBM and to select a tissue fragment with high content of viable tumor tissue. Each tissue specimen was minced into 1 mm^3 cubes and maintained in sterile saline at room temperature. Two to four cubes of the mincate were frozen on dry ice for extraction of RNA and DNA, and the remaining tissue was dissociated into a single cell suspension in media containing 0.2% collagenase, 0.01% hyaluronidase, and 0.002% DNaseI at 37°C for 30 to 60 min or at room temperature overnight.

Neurosphere Cultures

Neurosphere cultures were maintained in neurosphere culture medium (see Supplemental Experimental Procedures) in 3% oxygen and were passaged by trituration in nonenzymatic dissociation solution (Sigma, C-5914). All cultures were passaged when spheres reached approximately 200–300 microns in diameter, and cell counts were performed at the time of passage. For cultures passaged at intervals longer than one week, media containing fresh growth factors was added twice weekly.

To establish neurosphere cultures, dissociated tumor cells were seeded at an initial density of 1–5 × 10^5/ml. Sorted populations from each tumor case were matched for plating density.

FACS Analysis, Sorting, and Cloning

CD133 expression was monitored by use of CD133/1 Ab-PE (Miltenyi, cat. no. 130-080-801) either alone or in combination with CD133/2 Ab-PE (Miltenyi, cat. no. 130-090-853). For FACS analysis, all patient samples were analyzed within 24 hr of surgery and all cultures were analyzed at 6 days (±1 day) after passaging. FACS cloning was performed with a FACSAria sorter (BD Biosciences, San Jose, CA; see Figure S3). For each case, single cells were deposited into 192 wells of two 96-well plates. Microscopic examination confirmed that representative wells contained a single cell. Clones were scored by visual inspection of all wells at 3 to 4 weeks after seeding. Cutoff values of <1% and >10% were used for determination of absence and presence, respectively, of $CD133^+$ cells.

Western Blot

Six neurosphere lines and two adherent GBM lines, LN229 and U87 MG, were examined using PTEN antibody from Cell Signaling Technology (Danvers, MA).

Cell Aggregation Assays

Cells were suspended at a concentration of 2 × 10^6/ml in Hank's balanced salt solution containing 10 mM HEPES (pH 7.5), 1% bovine serum albumin, and either 1 mM calcium chloride plus 1 mM magnesium sulfate or 2 mM EDTA; 0.5 ml of cell suspensions were placed into wells of a 24-well culture plate and rotated on a gyratory shaker (100 rpm) at 37°C for 2 hr. Aggregation was terminated by the addition of 4% glutaraldehyde.

Differentiation of Clonal Cultures and Immunocytochemistry

To differentiate clonal neurosphere lines, dissociated cells were plated in eight-chamber slides at 5000 cells per well for 5 days in the neurobasal media (Invitrogen) supplemented with fetal bovine serum (10%; Sigma), B27 (1×; Invitrogen), L-glutamine (2 mM), penicillin (100 U/ml) and streptomycin (100 μl/ml; Invitrogen), dB-cAMP (100 μM; Sigma), and all-trans retinoic acid (0.5 μM; Sigma). For immunocytochemistry, primary antibodies were mouse anti-Nestin (1:200; Millipore), mouse anti-GalC, (1:150; Millipore), mouse anti-TUJ1 (1:1000; Covance), and mouse anti-GFAP-Alexa 488 (1:200; R&D System).

Orthotopic Grafts

Neurosphere cells (10^5) in 5 μl of Hanks balanced salt solution (Invitrogen) were stereotactically implanted unilaterally into the striatum of male CD1 nude mice. T2-weighted MR images were obtained using a 9.4-T magnet (Varian), and tumor volumes were calculated from resulting images using MRVision 1.5 software (Menlo Park, CA) by an observer blinded to experimental group. For serial transplantation, grafts were harvested and expanded for 1 to 2 weeks in neurosphere culture conditions prior to reimplantation. These studies were performed with the approval of Genentech's Institutional Animal Care and Use Committee. Genentech is accredited by AAALAC International, registered with the USDA, and follows the ILAR Guide for the Care and Use of Laboratory Animals.

Histology and Image Analysis

Histological analyses were performed on formalin fixed paraffin-embedded tissue sections. Antibodies for immunohistochemistry were as follows: CD133 (AbCam), FABP7 (AF3166 R&D Systems), Ki67 (M7240 Dako), and human Vimentin (AB8979, AbCam). MIB-1 indices in patient specimens (fraction $Ki67^+$ tumor cells) were determined by a neuropathologist using standard techniques. For quantification of the fraction of elongated and $Ki67^+$ cells in grafts, a modified TissueMap solution in Definiens Developer (version 7.0.4) was used to sample all nuclei present in the tumor tissue of one tissue section per animal.

DNA Analysis and Expression Profiling

DNA from patient tumors was profiled for copy number changes on Affymetrix 500k chips and sequenced for mutations in exons 4–8 of *p53* and exons 5 and 6 of *PTEN*. DNA from neurosphere lines was analyzed for copy number

alterations by profiling on Agilent 244K arrays. For expression profiling, RNA was extracted as described elsewhere (Phillips et al., 2006) and profiled on Agilent WHG (for patient samples) or WHG 4 × 44 chips (for neurosphere lines and grafts) according to the manufacturer's (Agilent technologies, Palo Alto CA) protocol. *Proneural*, *proliferative*, and *mesenchymal* GBM subtypes were determined by k means clustering of expression data from the Agilent WHG platform using a modification of the previously published 35 gene marker list (Phillips et al., 2006) (Table S1B). Principal component analysis was performed using Spotfire Decision Site software. For principal component analysis of SF6969 and GS-2 clonal cultures, probe sets (n = 156) included in the analysis were derived from a two-way ANOVA with tumor source and clone type as additive effects, implemented to detect common and significant (at a FDR of 1%) shifts across three clone types in both tumor sources studied.

Statistical Analysis

An alpha value of 0.05 was adopted for all analyses. All tests were two-tailed and corrected for multiple comparisons as appropriate. Details of the number of replicate observations and of statistical analysis are included in Supplemental Experimental Procedures.

ACCESSION NUMBERS

Microarray data have been deposited at GEO under accession number GSE19612.

SUPPLEMENTAL INFORMATION

Supplemental information includes six figures, eight tables, and Supplemental Experimental Procedures and may be found with this article online at doi:10.1016/j.ccr.2009.12.049.

ACKNOWLEDGMENTS

We thank M. Baatz and J. Zimmermann for implementation of the image analysis solution; J. Eastham-Anderson and J. Zha for assistance with histological analysis; T. Le, W. Tombo, and J. Ayers for expert technical assistance; J. Cupp for FACS consultation; A. Bruce for graphics; T. Wu for bioinformatics support; and G. Plowman for helpful discussions. This study was supported by the State of California and the University of California Industry-University Cooperative Research Discovery (grant Bio05-10501), the National Brain Tumor Society (support to J.F.C. and S.M.), and by the National Institutes of Health (grant CA 097257 to C.D.J., S.R.V., and M.D.P.). R.C., M.C.N., S.M.B., S.K., W.F.F., I.M.K., J.M.G., R.H.S., L.L.G., C.S.R., Z.M., S.N., S.G., K.A.E., J.J.W., and H.S.P. are employees of Genentech, Inc., a member of the Roche group. This work was supported in part by a grant from Genentech to C.D.J., S.R.V., J.F.C., S.M., M.P., and C.C. M.P. has received research grant support from Genentech for clinical trials that were not related in any way with the research described in this manuscript.

Received: April 14, 2009
Revised: September 30, 2009
Accepted: February 8, 2010
Published: April 12, 2010

REFERENCES

Alcantara Llaguno, S., Chen, J., Kwon, C.-H., Jackson, E.L., Li, Y., Burns, D.K., Alvarez-Buylla, A., and Parada, L.F. (2009). Malignant astrocytomas originate from neural stem/progenitor cells in a somatic tumor suppressor mouse model. Cancer Cell *15*, 45–56.

Arai, Y., Funatsu, N., Numayama-Tsuruta, K., Nomura, T., Nakamura, S., and Osumi, N. (2005). Role of Fabp7, a downstream gene of Pax6, in the maintenance of neuroepithelial cells during early embryonic development of the rat cortex. J. Neurosci. *25*, 9752–9761.

Bao, S., Wu, Q., Sathornsumetee, S., Hao, Y., Li, Z., Hjelmeland, A.B., Shi, Q., McLendon, R.E., Bigner, D.D., and Rich, J.N. (2006). Stem cell-like glioma cells promote tumor angiogenesis through vascular endothelial growth factor. Cancer Res. *66*, 7843–7848.

Beier, D., Hau, P., Proescholdt, M., Lohmeier, A., Wischhusen, J., Oefner, P.J., Aigner, L., Brawanski, A., Bogdahn, U., and Beier, C.P. (2007). CD133(+) and CD133(-) glioblastoma-derived cancer stem cells show differential growth characteristics and molecular profiles. Cancer Res. *67*, 4010–4015.

Bleau, A.M., Hambardzumyan, D., Ozawa, T., Fomchenko, E.I., Huse, J.T., Brennan, C.W., and Holland, E.C. (2009). PTEN/PI3K/Akt pathway regulates the side population phenotype and ABCG2 activity in glioma tumor stem-like cells. Cell Stem Cell *4*, 226–235.

Clarke, M.F., Dick, J.E., Dirks, P.B., Eaves, C.J., Jamieson, C.H., Jones, D.L., Visvader, J., Weissman, I.L., and Wahl, G.M. (2006). Cancer stem cells—perspectives on current status and future directions: AACR Workshop on cancer stem cells. Cancer Res. *66*, 9339–9344.

Dai, C., Celestino, J.C., Okada, Y., Louis, D.N., Fuller, G.N., and Holland, E.C. (2001). PDGF autocrine stimulation dedifferentiates cultured astrocytes and induces oligodendrogliomas and oligoastrocytomas from neural progenitors and astrocytes in vivo. Genes Dev. *15*, 1913–1925.

Galli, R., Binda, E., Orfanelli, U., Cipelletti, B., Gritti, A., De Vitis, S., Fiocco, R., Foroni, C., Dimeco, F., and Vescovi, A. (2004). Isolation and characterization of tumorigenic, stem-like neural precursors from human glioblastoma. Cancer Res. *64*, 7011–7021.

Ghashghaei, H.T., Weimer, J.M., Schmid, R.S., Yokota, Y., McCarthy, K.D., Popko, B., and Anton, E.S. (2007). Reinduction of ErbB2 in astrocytes promotes radial glial progenitor identity in adult cerebral cortex. Genes Dev. *21*, 3258–3271.

Gregorian, C., Nakashima, J., Le Belle, J., Ohab, J., Kim, R., Liu, A., Smith, K.B., Groszer, M., Garcia, A.D., Sofroniew, M.V., et al. (2009). Pten deletion in adult neural stem/progenitor cells enhances constitutive neurogenesis. J. Neurosci. *29*, 1874–1886.

Groszer, M., Erickson, R., Scripture-Adams, D.D., Lesche, R., Trumpp, A., Zack, J.A., Kornblum, H.I., Liu, X., and Wu, H. (2001). Negative regulation of neural stem/progenitor cell proliferation by the Pten tumor suppressor gene in vivo. Science *294*, 2186–2189.

Gunther, H.S., Schmidt, N.O., Phillips, H.S., Kemming, D., Kharbanda, S., Soriano, R., Modrusan, Z., Meissner, H., Westphal, M., and Lamszus, K. (2008). Glioblastoma-derived stem cell-enriched cultures form distinct subgroups according to molecular and phenotypic criteria. Oncogene *27*, 2897–2909.

Iulianella, A., Sharma, M., Durnin, M., Vanden Heuvel, G.B., and Trainor, P.A. (2008). Cux2 (Cutl2) integrates neural progenitor development with cell-cycle progression during spinal cord neurogenesis. Development *135*, 729–741.

Jaksch, M., Munera, J., Bajpai, R., Terskikh, A., and Oshima, R.G. (2008). Cell cycle-dependent variation of a CD133 epitope in human embryonic stem cell, colon cancer, and melanoma cell lines. Cancer Res. *68*, 7882–7886.

Joo, K.M., Kim, S.Y., Jin, X., Song, S.Y., Kong, D.-S., Lee, J.-I., Jeon, J.W., Kim, M.H., Kang, B.G., Jung, Y., et al. (2008). Clinical and biological implications of CD133-positive and CD133-negative cells in glioblastomas. Lab. Invest. *88*, 808–815.

Kaloshi, G., Mokhtari, K., Carpentier, C., Taillibert, S., Lejeune, J., Marie, Y., Delattre, J.-Y., Godbout, R., and Sanson, M. (2007). FABP7 expression in glioblastomas: relation to prognosis, invasion and EGFR status. J. Neurooncol. *84*, 245–248.

Korkaya, H., and Wicha, M.S. (2007). Selective targeting of cancer stem cells: a new concept in cancer therapeutics. Biodrugs *21*, 299–310.

Kwon, C.-H., Zhao, D., Chen, J., Alcantara, S., Li, Y., Burns, D.K., Mason, R.P., Lee, E.Y.H.P., Wu, H., and Parada, L.F. (2008). Pten haploinsufficiency accelerates formation of high-grade astrocytomas. Cancer Res. *68*, 3286–3294.

Liang, Y., Bollen, A.W., Aldape, K.D., and Gupta, N. (2006). Nuclear FABP7 immunoreactivity is preferentially expressed in infiltrative glioma and is associated with poor prognosis in EGFR-overexpressing glioblastoma. BMC Cancer *6*, 97.

Nieto, M., Monuki, E.S., Tang, H., Imitola, J., Haubst, N., Khoury, S.J., Cunningham, J., Gotz, M., and Walsh, C.A. (2004). Expression of Cux-1 and

Cux-2 in the subventricular zone and upper layers II-IV of the cerebral cortex. J. Comp. Neurol. *479*, 168–180.

Noctor, S.C., Martinez-Cerdeno, V., and Kriegstein, A.R. (2007). Contribution of intermediate progenitor cells to cortical histogenesis. Arch. Neurol. *64*, 639–642.

Ogden, A.T., Waziri, A.E., Lochhead, R.A., Fusco, D., Lopez, K., Ellis, J.A., Kang, J., Assanah, M., McKhann, G.M., Sisti, M.B., et al. (2008). Identification of A2B5+CD133- tumor-initiating cells in adult human gliomas. Neurosurgery *62*, 505–514; discussion 514–505.

Pallini, R., Ricci-Vitiani, L., Banna, G.L., Signore, M., Lombardi, D., Todaro, M., Stassi, G., Martini, M., Maira, G., Larocca, L.M., and De Maria, R. (2008). Cancer stem cell analysis and clinical outcome in patients with glioblastoma multiforme. Clin. Cancer Res. *14*, 8205–8212.

Phillips, H.S., Kharbanda, S., Chen, R., Forrest, W.F., Soriano, R.H., Wu, T.D., Misra, A., Nigro, J.M., Colman, H., Soroceanu, L., et al. (2006). Molecular subclasses of high-grade glioma predict prognosis, delineate a pattern of disease progression, and resemble stages in neurogenesis. Cancer Cell *9*, 157–173.

Read, T.-A., Fogarty, M.P., Markant, S.L., McLendon, R.E., Wei, Z., Ellison, D.W., Febbo, P.G., and Wechsler-Reya, R.J. (2009). Identification of CD15 as a marker for tumor-propagating cells in a mouse model of medulloblastoma. Cancer Cell *15*, 135–147.

Sakariassen, P.Ø., Immervoll, H., and Chekenya, M. (2007). Cancer stem cells as mediators of treatment resistance in brain tumors: status and controversies. Neoplasia *9*, 882–892.

Schuller, U., Heine, V.M., Mao, J., Kho, A.T., Dillon, A.K., Han, Y.-G., Huillard, E., Sun, T., Ligon, A.H., Qian, Y., et al. (2008). Acquisition of granule neuron precursor identity is a critical determinant of progenitor cell competence to form Shh-induced medulloblastoma. Cancer Cell *14*, 123–134.

Singh, S.K., Hawkins, C., Clarke, I.D., Squire, J.A., Bayani, J., Hide, T., Henkelman, R.M., Cusimano, M.D., and Dirks, P.B. (2004). Identification of human brain tumour initiating cells. Nature *432*, 396–401.

Taylor, M.D., Poppleton, H., Fuller, C., Su, X., Liu, Y., Jensen, P., Magdaleno, S., Dalton, J., Calabrese, C., Board, J., et al. (2005). Radial glia cells are candidate stem cells of ependymoma. Cancer Cell *8*, 323–335.

Uhrbom, L., Dai, C., Celestino, J.C., Rosenblum, M.K., Fuller, G.N., and Holland, E.C. (2002). Ink4a-Arf loss cooperates with KRas activation in astrocytes and neural progenitors to generate glioblastomas of various morphologies depending on activated Akt. Cancer Res. *62*, 5551–5558.

Wang, J., Sakariassen, P.O., Tsinkalovsky, O., Immervoll, H., Boe, S.O., Svendsen, A., Prestegarden, L., Rosland, G., Thorsen, F., Stuhr, L., et al. (2008). CD133 negative glioma cells form tumors in nude rats and give rise to CD133 positive cells. Int. J. Cancer *122*, 761–768.

Wei, Q., Clarke, L., Scheidenhelm, D.K., Qian, B., Tong, A., Sabha, N., Karim, Z., Bock, N.A., Reti, R., Swoboda, R., et al. (2006). High-grade glioma formation results from postnatal pten loss or mutant epidermal growth factor receptor expression in a transgenic mouse glioma model. Cancer Res. *66*, 7429–7437.

Xiao, A., Wu, H., Pandolfi, P.P., Louis, D.N., and Van Dyke, T. (2002). Astrocyte inactivation of the pRb pathway predisposes mice to malignant astrocytoma development that is accelerated by PTEN mutation. Cancer Cell *1*, 157–168.

Yang, Z.-J., Ellis, T., Markant, S.L., Read, T.-A., Kessler, J.D., Bourboulas, M., Schuller, U., Machold, R., Fishell, G., Rowitch, D.H., et al. (2008). Medulloblastoma can be initiated by deletion of Patched in lineage-restricted progenitors or stem cells. Cancer Cell *14*, 135–145.

Zheng, H., Ying, H., Yan, H., Kimmelman, A.C., Hiller, D.J., Chen, A.-J., Perry, S.R., Tonon, G., Chu, G.C., Ding, Z., et al. (2008). p53 and Pten control neural and glioma stem/progenitor cell renewal and differentiation. Nature *455*, 1129–1133.